

Exploring intermolecular interactions in some halogen substituted formyl coumarins and their DFT studies

Gulab Singh^{a*}, Khalid Hussain^b and Rekha Gaba^c

^aDepartment of Chemistry, SUS Govt. College, Matak Majri, Karnal-132041, India

^bDepartment of Applied Sciences and Humanities, Mewat engineering college, Nuh, Mewat-122107, India

^cDepartment of Chemistry, DAV university Jalandhar, Punjab-144001, India

CHRONICLE

Article history:

Received June 27, 2021

Received in revised form

July 19, 2021

Accepted November 11, 2021

Available online

November 11, 2021

Keywords:

NBO

NLO

Hirshfeld Surface

2D fingerprint

HOMO

LUMO

ABSTRACT

The present manuscript describes an in-depth analysis of various interactions present in the crystal structure of formyl coumarins using Crystal explorer 17.0. Element based interactions were quantified by the decomposition of generated 3D surfaces into 2D fingerprint regions. DFT methods were used to explore electrostatic parameters, global and local reactivity descriptors. Electrophilicity based charge transfer (ECT) analysis was done to explore the probability of charge transfer between formyl coumarins and DNA base pairs. The reactivity and selectivity of different formyl coumarins have been accessed using Fukui functions in their reduced form. Non-bonding orbital (NBO) analysis revealed the presence of various hyperconjugative interactions and their stabilization energy in formyl coumarins. Non-linear optical properties are presented in terms of first order hyperpolarizability (β_0), where maximum β_0 is observed for C4 (1.64×10^{-30} esu.) which is found to be 2 times greater than that of *p*-nitroaniline. Molecular electrostatic potential (MEP) plots are mapped in terms of electron density.

© 2022 by the authors; licensee Growing Science, Canada.

1. Introduction

Exploring intermolecular and intramolecular interactions using theoretical methods has always been an area of attraction for chemists, as it opens new horizons in the field of structural chemistry. The study of intermolecular interactions is an emerging area in crystal engineering¹. Supramolecular assembly of molecules depends to a great extent on the presence of non-covalent interactions such as aromatic π -stacking, strong and directional hydrogen bonds^{2,3}. Functional groups like carbonyl, amino and ester, play a significant role in supramolecular assemblies *via* repetitive hydrogen bonds⁴. The constituents participating in supramolecular architecture should possess more than two complementary sites in terms of strong and directional hydrogen bonds⁵. Nature sets a beautiful example of maintaining integrity in bio-molecular structures by exploiting⁶ the complementarities between hydrogen bonded systems^{6,7}. Appropriate programming of complementarities between molecular species resulted in linear as well as non-linear arrays in supramolecular architectures. Multiple non-covalent interactions is possible in compounds which are highly symmetrical, rigid and hold interactive groups together⁸. The Hirshfeld surface is an invaluable tool for quantitative analysis of molecular properties and provides an insight into the crystal packing behaviors. With its development, the barrier in the exploration of molecular interactions and their direct environment has been removed⁹⁻¹¹. Moreover, molecular fingerprint allows comparative analysis of molecules in different environments¹².

* Corresponding author.

E-mail address: gulabsingh2007@gmail.com (G. Singh)

Density functional theory (DFT) has been established as a vibrant tool in computational chemistry for determining molecular structure and predicting electrostatic properties^{13–15}. Investigation of reaction kinetics, proton affinities and catalytic sites of a molecule can equally be possible using DFT based quantum calculations^{16–19}. Recently, DFT based methods have been extensively applied to both micro and macromolecular structures²⁰. The DFT based global reactivity descriptors has been extensively utilized in the development of QSAR in biological systems^{21–23}. Moreover, the spectral properties *i.e.*, vibrational spectra and NMR spectra have been explored for a diverse library of organic and inorganic compounds^{24–26}. The non-linear optical properties of a molecule can be assessed by means of hyper-polarizabilities calculated using DFT based methods^{19,27}.

In view of the above discussed facts, we have explored the detailed intermolecular interactions using the Hirshfeld surface, molecular fingerprint for halogen substituted formyl coumarins. Moreover, the electrostatic properties, NBO and NLO associated with these molecules have been explored using DFT based methods.

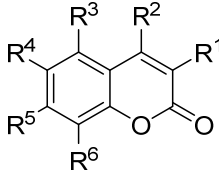
2. Results and discussion

2.1 Crystal studies

Halogen substituted formyl coumarins selected for the present study have been retrieved from the crystallographic center for data collection (CCDC) using CCDC number. The substitution pattern and their position in different halogen substituted formyl coumarins have been shown in **Table 1**.

Table 1. Substitution pattern of halogen substituted formyl coumarins (C1–C6)

Compound	R ¹	R ²	R ³	R ⁴	R ⁵	R ⁶
C1	H	CHO	H	H	H	H
C2	H	CHO	H	Cl	H	H
C3	H	CHO	H	H	Cl	H
C4	H	CHO	H	H	Br	H
C5	H	CHO	H	F	H	H
C6	H	CHO	H	H	F	H



2.2 Hirshfeld surface

Hirshfeld surface (HS) analysis is a useful tool, which defines molecular volume similar to van der Waal (vdW) surfaces and used for exploring surface characteristics, H-bonding and close contacts in a quantitative manner. The crystallographic information retrieved from CCDC utilized as input for surface analysis using crystal explorer 17.0²⁸. In order to explore H-bonding, close contacts and various intermolecular interactions quantitatively, the HS analysis of the formyl coumarin derivatives (C1 to C6) has been done (**Fig. 1**). HS can be mapped in the form of d_e and d_i , which signifies the distance of internal or external atoms from the mapped surface respectively. One more parameter, d_{norm} results from the normalization of d_e and d_i with respect to vdW radii. Color-coding has been used for various intermolecular interactions in HS surfaces. Negative d_{norm} are highlighted by red color indicating distance shorter than vdW radii, positive d_{norm} values are highlighted by dark blue color indicating distance larger than vdW radii. However, d_{norm} values highlighted in white represent distance close to vdW radii (**Table 2**). The molecular structure is visualized in a transparent manner in all HS.

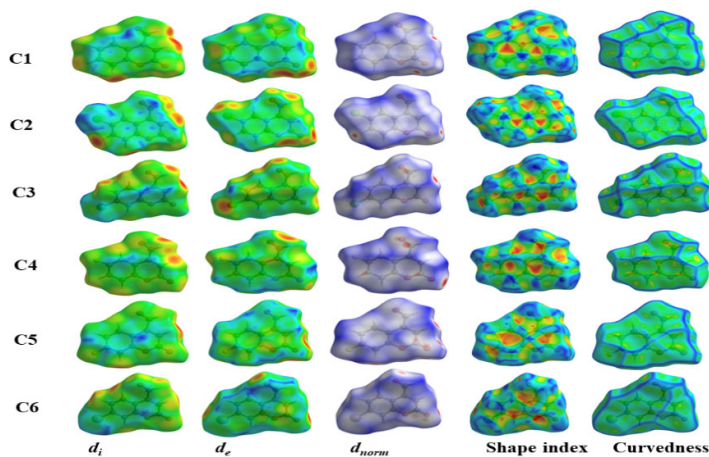


Fig. 1. Hirshfeld Surface analysis of halogen substituted formyl coumarins (C1 to C6)

The same range of d_i and d_e in these entire molecules reflects the presence of good close packing and strong intermolecular interactions.

Table 2. Hirshfeld Surface parameters for formyl coumarins (C1-C6)

Compound	$d_i(\text{Å})$	$d_e(\text{Å})$	$d_{\text{norm}}(\text{Å})$	Shape index	Curvedness
C1	1.058-2.408	1.059-2.275	-0.107-1.119	-0.998-0.999	-3.602-0.55
C2	1.067-2.309	1.069-2.407	-0.109-1.183	-0.980-0.997	-3.884-0.208
C3	0.980-2.467	0.981-2.574	-0.243-1.074	-0.992-0.998	-3.458-0.095
C4	0.915-2.629	0.916-2.507	-0.339-1.153	-0.992-0.998	-4.293-0.216
C5	1.042-2.569	1.046-2.414	-0.192-0.982	-0.987-0.996	-3.375-0.223
C6	0.975-2.438	0.974-2.341	-0.246-1.088	-0.992-0.997	-3.814-0.215

The Hirshfeld surface has been decomposed into 2D fingerprint in order to explore the various possible contacts in different coumarin derivatives (C1 to C6). The 2D fingerprint along with their element-based decomposition of % interaction has been shown in Fig. 2.

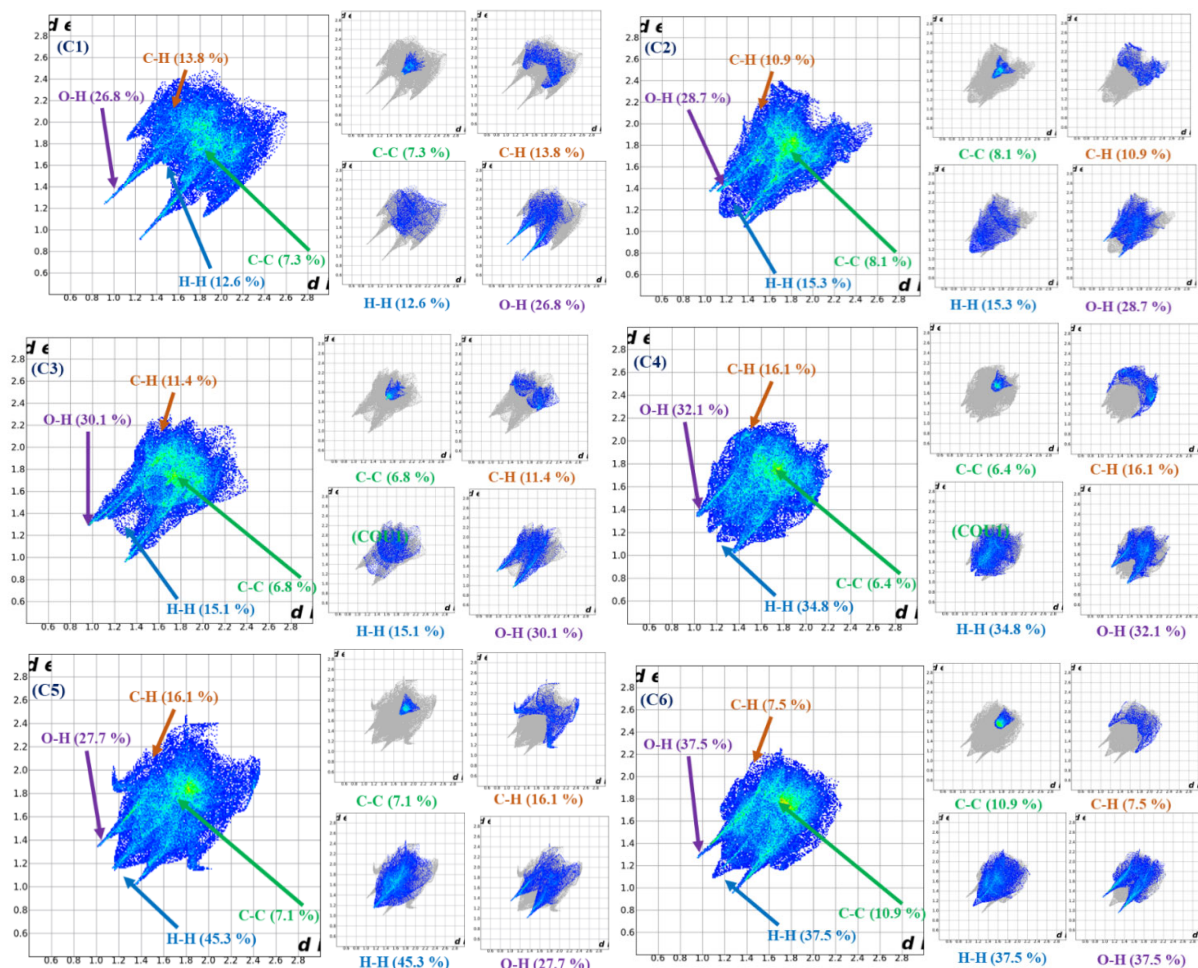


Fig. 2. 2D fingerprint analysis of formyl coumarin derivatives (C1 to C6)

Two different patterns have been observed in case of different formyl coumarins (C1 to C6). In case of first three coumarins *i.e.*, C1, C2 and C3, O-H interaction is the most significant one with 26.8, 28.7 and 30.1% contribution in the overall interaction respectively. However, in the next two molecules *i.e.*, C4 and C5, H-H interaction is the most significant one with a contribution of 34.8 and 45.3 % respectively. As far as C6 is concerned the contribution of both H-H and O-H interactions is the same *i.e.*, 37.5%. The presence of strong O-H interactions in all the six cases revealed the presence of strong non-covalent hydrogen bonding. The percentage of O-H interaction increases as the halogen atom moves away from the formyl group. The other interactions, C-H, and C-C interactions also have significant contributions towards the total Hirshfeld surface (Fig. 2).

2.2 DFT Studies

2.2.1 Electrostatic results

HOMO and LUMO are the most important orbitals also known as Frontier molecular orbitals (FMOs), and energy related with them can be utilized to access the reactivity of a molecule. HOMO determines the ability of electron donation, however LUMO determines the ability of electron acceptance. HOMO and LUMO orbitals are examined for all the six-formyl coumarins and shown in **Fig. 3** to **Fig. 8**. The distribution of electrons reflects the accepting and donating ability of atoms within a molecule, which can be assessed using HOMO and LUMO orbitals. The energy values of these orbitals are used to calculate the Ionization Potential (IP) and Electron Affinity (EA) by following formulas:

$$EA = -E_{\text{LUMO}} \quad (1)$$

$$IP = -E_{\text{HOMO}} \quad (2)$$

The chemical hardness (H), chemical softness (s), Electronegativity (χ), electrophilicity index (ω) and chemical potential (μ) are calculated by using ionization potential and electron affinity in following formulas^{13,29,30}:

$$\chi = -\mu = (IP + EA)/2 \quad (3)$$

$$H = (IP - EA)/2 \quad (4)$$

$$s = 1/H \quad (5)$$

$$\omega = \mu^2/2H \quad (6)$$

Global reactivity descriptors calculated for all the six-formyl coumarins have been tabulated in **Table 3**. The molecules with high ΔE value are chemically stable due to difficulty in their polarization. According to Pearson, molecules associated with high ΔE value are chemically hard and are more stable than soft molecules with low ΔE value. The large values of IP reflect the strong ability of electron donation and the large value of EA indicates the strong ability of electron acceptance. The high IP value associated with six all formyl coumarins (C1-C6) represent high electron donating tendency and electrophilicity index. The stability and hardness of a molecule can also be ascertained using ΔE value *i.e.*, HOMO-LUMO. Higher the value of ΔE , higher is the stability and hardness associated with them. All the six formyl-substituted coumarins (C1-C6) are chemically stable. It has been revealed from the results mentioned in **Table 3**, fluorine substituted formyl coumarin (C6) is the most hardest among all followed by C1. The effect of substituent position does have a substantial effect on the chemical hardness and softness of different formyl coumarins (C1-C6). Compounds substituted with chlorine and fluorine at 7th position of coumarin ring are more-harder than those having these substituents on 6th position. Similar pattern of softness was observed for all the substituted coumarin derivatives (**Table 3**). The HOMO-LUMO gap for all the coumarin derivatives was also calculated in different solvents of varying polarity. It is worth mentioning here that no significant effect in the ΔE value was observed when the calculation was attempted in solvents of varying polarity (**Fig. 3- Fig. 8**).

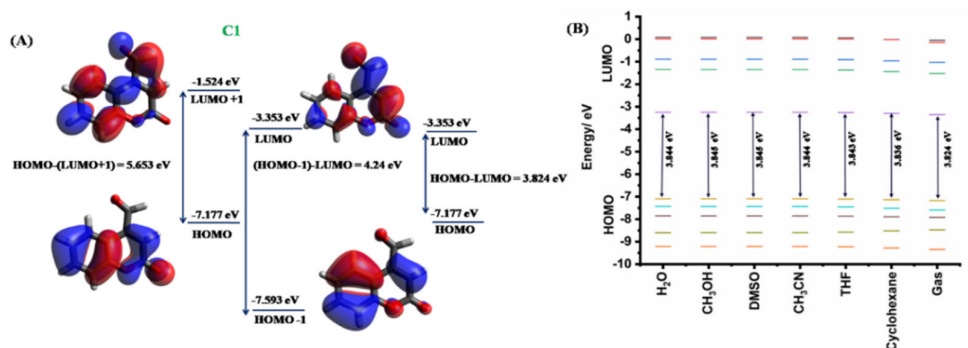


Fig. 3. (A) FMO analysis of C1; (B) Density of state analysis for C1

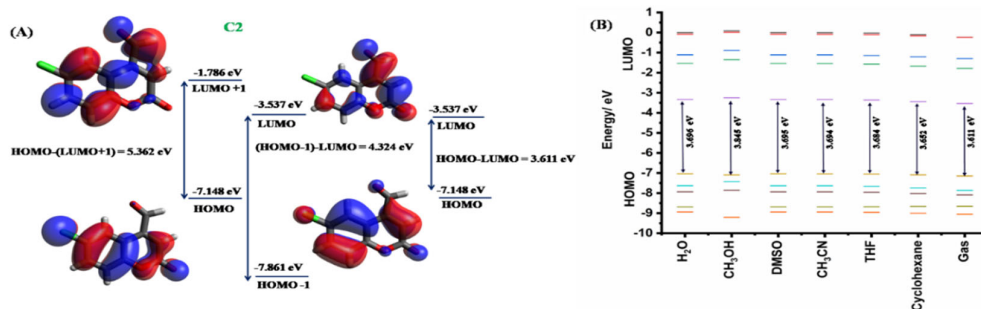


Fig. 4. (A) FMO analysis of C2; (B) Density of state analysis for C2

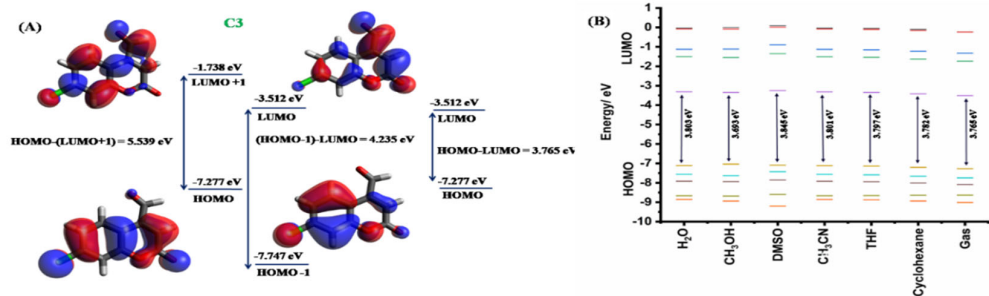


Fig. 5. (A) FMO analysis of C3; (B) Density of state analysis for C3

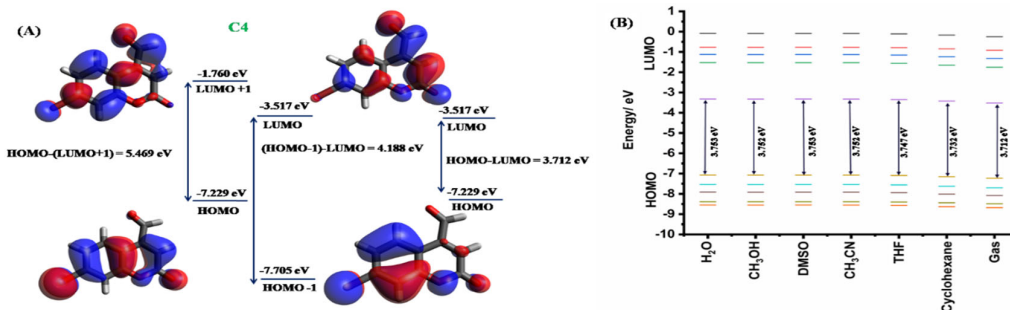


Fig. 6. (A) FMO analysis of C4; (B) Density of state analysis for C4

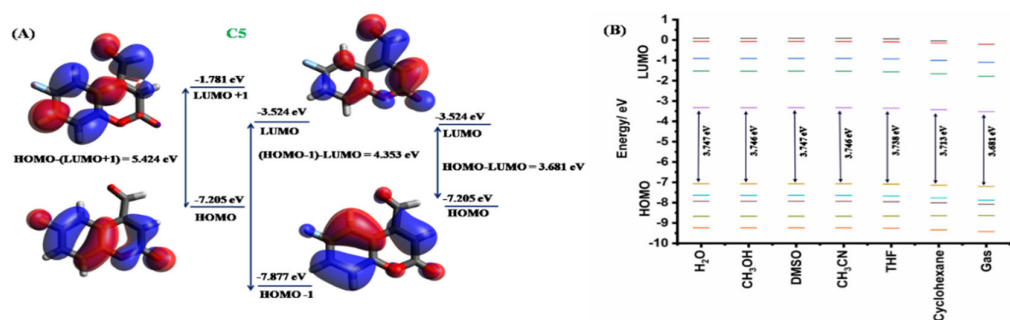


Fig. 7. (A) FMO analysis of C5; (B) Density of state analysis for C5

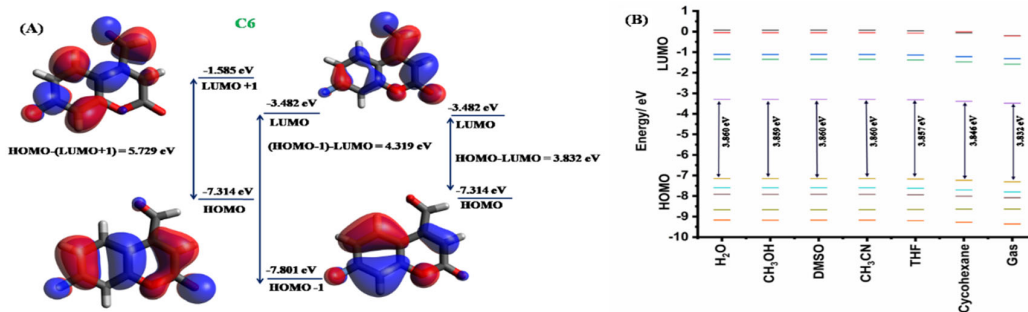


Fig. 8. (A) FMO analysis of C6; (B) Density of state analysis for C6

Table 3. Electrostatic results of differently substituted coumarin derivatives (C1-C6)

Compound	HOMO	LUMO	Electronegativity (χ)= (IP+EA)/2	Chemical Potential (μ)	Chemical Hardness (η)=(IP-EA)/2	Chemical Softness $\sigma=1/\eta$	Electrophilicity Index
C1	-7.177	-3.353	5.265	-5.265	1.912	0.262	7.249
C2	-7.148	-3.537	5.343	-5.343	1.806	0.277	7.904
C3	-7.277	-3.512	5.395	-5.395	1.883	0.266	7.729
C4	-7.229	-3.517	5.373	-5.373	1.856	0.269	7.777
C5	-7.205	-3.524	5.365	-5.365	1.841	0.272	7.818
C6	-7.314	-3.482	5.398	-5.398	1.916	0.261	7.604

In order to calculate the absorption spectra of all the compounds (C1-C6), TD-DFT calculations were performed for all the molecules using the same level of theory as used for ground state optimization of the molecules. The calculated absorption spectra for all the compounds is presented in Fig. 9.

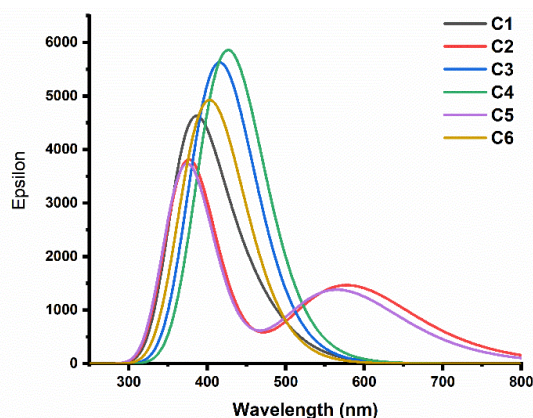


Fig. 9. Absorption spectra using TD-DFT calculation for C1-C6

The concept of vertical and adiabatic ionization potential and electron affinity varies with the nature of the computational method employed in the study. According to Koopman's theory, the eigenvalues of orbitals correspond to measurable quantities where the values of HOMO and LUMO are vertical ionization potential and electron affinity, respectively. However, this is not necessarily the case with DFT based methods, since corrections are required for Kohn-Sham HOMO orbitals to reproduce ionization potential. In an attempt to calculate the adiabatic ionization potential (IP_A) and electron affinity (EA_A) for substituted coumarin derivatives. The structure of neutral, cationic and anionic coumarin derivatives (C1-C6) has been optimized using B3LYP/6-311G(+),d,p and CAM-B3LYP/6-311G(+),d,p level of theory, and their respective ionization potential and electron affinity was calculated using ΔE method (Table 4). The following equations are used for IP_A and EA_A .

$$IP_A = E^0 - E^+ \quad (7)$$

$$EA_A = E^- - E^0 \quad (8)$$

Table 4: Adiabatic ionization potential and electron affinity calculated using ΔE method

Compound	B3LYP/6-311G(+),d,p		CAM-B3LYP/6-311G(+),d,p	
	Ionization potential (eV)	Electron affinity (eV)	Ionization potential (eV)	Electron affinity (eV)
C1	-8.799	-1.854	-8.898	-1.813
C2	-8.672	-2.072	-8.806	-2.028
C3	-8.825	-2.055	-8.965	-2.015
C4	-20.456	9.622	-8.922	-2.032
C5	-8.786	-2.030	-8.885	-1.990
C6	-8.927	-1.993	-9.032	-1.955

It has been revealed from above results that a consistency in IP_A and EA_A was observed when CAM-B3LYP/6-311G(+),d,p level of theory was used. Electrophilicity index (ω) defines the stability of a system when additional electronic charge has been added to it³¹. The direction of charge transfer in a molecular system can be ascertained by examining the value of chemical potential (μ), and hence negative value of chemical potential represents electrophilicity.

Table 5. Electrophilicity based charge transfer (ECT) analysis of halogen substituted formyl coumarins

Compound	Ionization potential	Electron affinity	Chemical potential (μ)	Chemical hardness (η)= (IP-EA)/2	ΔN_{max}	ECT for adenine	ECT for cytosine	ECT for Thymine	ECT for guanine
C1	-8.898	-1.813	-5.356	-3.543	1.512	0.519	0.643	0.586	0.578
C2	-8.806	-2.028	-5.417	-3.389	1.598	0.605	0.730	0.673	0.664
C3	-8.965	-2.015	-5.490	-3.475	1.580	0.587	0.711	0.654	0.646
C4	-8.922	-2.032	-5.477	-3.445	1.590	0.597	0.721	0.664	0.656
C5	-8.885	-1.990	-5.438	-3.448	1.577	0.584	0.708	0.652	0.643
C6	-9.032	-1.955	-5.494	-3.539	1.552	0.559	0.684	0.627	0.618
Adenine	-8.306	0.029	-4.139	-4.168	0.993				
Cytosine	-8.737	0.613	-4.062	-4.675	0.869				
Guanine	-9.047	0.350	-4.349	-4.699	0.926				
Thymine	-9.506	0.324	-4.591	-4.915	0.934				

In an electron transfer reaction, species with lower electrophilicity index represent nucleophilic behavior. In order to explore the direction of charge transfer, electrophilicity charge transfer (ECT) index was calculated for formyl coumarins and compared with DNA base pairs, ECT is defined as the difference between ΔN_{max} value of interacting molecules. The greater nucleophilic behavior of DNA base pair over formyl coumarins (**C1-C6**) have been revealed from **Table 5**. Both coumarin derivatives and DNA base pairs are marked as **A** and **B** respectively. Two possibilities result when both **A** and **B** approaches closer to **B**; (i) **B** behaves nucleophilically when $ECT > 0$. (ii) **A** behaves nucleophilically when $ECT < 0$.

$$ECT = (\Delta N_{max})_A - (\Delta N_{max})_B$$

where $(\Delta N_{max})_A = \mu_A/\eta_A$ and $(\Delta N_{max})_B = \mu_B/\eta_B$.

Fukui function represents a local reactivity descriptor which accesses the selectivity and reactivity of a molecule under consideration^{32, 33}. Electron density distortion within a molecule on gain or loss of electrons and these sites prone to nucleophilic, electrophilic and radical attack can be assessed. The condensed form of these functions can be used at atomic level and expressed as for radical, electrophilic and nucleophilic attack respectively as mentioned below:

$$f_x^+ = q^x(N+1) - q^x(N)$$

$$f_x^- = q^x(N) - q^x(N-1)$$

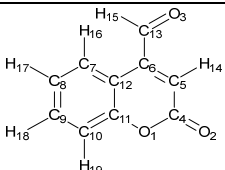
$$f_x^0 = (q^x(N+1) - q^x(N-1))/2$$

In the above expressions, $q^x(N-1)$, $q^x(N+1)$ and $q^x(N)$ chemical species represents the electronic population for x^{th} atom in anionic, cationic and neutral atom. The natural charge on each atom can be accessed using NBO analysis. Electron rich and electron deficient sites can be differentiated within a molecule using $f(r)$ a dual descriptor $f(r)$ proposed by Morrel *et al.*

$$\Delta f(r) = (f_x^+ - f_x^-)$$

The electrophilic centres are represented by $\Delta f(r) > 0$, while nucleophilic centres by $\Delta f(r) < 0$. The Fukui functions calculated for different coumarin derivatives (**C1-C6**) are summarised in **Table 6**. The results obtained from Fukui function calculation give an idea of different electrophilic and nucleophilic centres present in case of differently substituted coumarin derivatives (C1-C6). In case of **C1**, the C4 carbon is susceptible for nucleophilic attack since it has $\Delta f(r)$ value of -1.475. However, the C5 carbon is susceptible for electrophilic attack with a $\Delta f(r)$ value of 0.376. As far as other carbon centres of fused benzene ring is concerned, C7 and C10 are more electrophilic than C8 and C9 carbon atoms. The effect of different halogen atoms and their position also effects the electrophilic and nucleophilic behaviours of respective carbon centres. It is noteworthy to mention here that among halogen substituted coumarin derivatives, C5 carbon is more electrophilic due to the presence of chlorine at C8 carbon. However, substituting the same position with fluorine didn't affect the electrophilic behaviour of C5 significantly. The presence of different halogens on C9 carbon resulted into decrease in electrophilic character of C5 which might be attributed due to the presence of resonance effects in these cases. Similarly, the presence of these halogens affects the nucleophilic character of C4, which is highest in case of compound **C2**.

Table 6. Condensed Fukui function for substituted coumarin derivatives (**C1-C6**)

Compound	Atoms	Δf					
		C1	C2	C3	C4	C5	C6
	O ₁	0.945	0.958	0.975	0.980	0.952	0.968
	O ₂	0.911	0.935	0.929	0.939	0.920	0.914
	O ₃	0.953	0.984	0.976	0.979	0.976	0.972
	C ₄	-1.475	-1.494	-1.489	-1.490	-1.491	-1.487
	C ₅	0.376	0.384	0.345	0.348	0.374	0.346
	C ₆	0.139	0.145	0.148	0.155	0.144	0.140
	C ₇	0.325	0.364	0.298	0.315	0.458	0.311
	C ₈	0.268	0.011	0.330	0.332	-0.939	0.389
	C ₉	0.253	0.311	-0.015	0.144	0.377	-0.966
	C ₁₀	0.453	0.397	0.496	0.497	0.395	0.589
	C ₁₁	-0.805	-0.787	-0.762	-0.752	-0.778	-0.778
	C ₁₂	0.174	0.187	0.149	0.133	0.168	0.154
	C ₁₃	-0.828	-0.826	-0.823	-0.824	-0.823	-0.822
	H ₁₄	-0.491	-0.495	-0.494	-0.493	-0.497	-0.496
	H ₁₅	-0.264	-0.293	-0.294	-0.293	-0.295	-0.296
	H ₁₆	-0.518	-0.555	-0.535	-0.536	-0.562	-0.537
	H ₁₇	-0.460		-0.483	-0.481		-0.490
	H ₁₈	-0.462	-0.487			-0.494	
	H ₁₉	-0.496	-0.498	-0.515	-0.513	-0.499	-0.523
	X ₂₀		-0.240	-0.235	-0.438	0.612	0.612

NBO is one of the best methods for exploring the characteristics of a chemical bond due to its remarkable numerical stability and convergence³⁴. Inter and intramolecular interactions present between suitable bonding and non-bonding orbitals in molecules can be explored in a qualitative manner by NBO analysis [35]. NBO analysis gives the probability of charge transfer between different orbitals by exploring various hyperconjugative interactions in a molecule. Furthermore, the extent of H-bonding can be predicted by using the stabilization energy of different transitions. Stabilization energy can be further used to predict the stability of H-bonding. The intensity of interaction between electron donor and acceptor depends on the value of stabilization energy. The intermolecular interactions in different halogen substituted formyl coumarins has been explored using second order Fock matrix perturbation theory using the level of theory as was used for the optimization of the structures. Full NBO analysis was done on all the molecules to explore the composition of hybrid orbitals ($sp^x d^y$) in a chemical bond.

The hyperconjugative interaction was explored using a second order Fock matrix, where the value of $E(2)$ shows the intensity of interaction between electron-donors and electron-acceptors³⁶. The extent of conjugation in the whole system is governed by the donating tendency from electron donors to electron acceptors. It has been revealed from second order Fock analysis that three types of interactions are more significant in case of all the molecules *i.e.*, π to π^* , n to σ^* and n to π^* . In case of π to π^* the most intense transitions in case of **C1** is from πC_5-C_6 to $\pi^* O_2-C_4$ with a stabilization energy of 15.51 Kcal/mol. In case of all other molecules the same π to π^* interaction exists between the same bonds as present in case of **C1**. The interaction energy for this interaction in **C2**, **C3**, **C4**, **C5** and **C6** are 15.38, 15.47, 15.47, 15.40 and 15.52 Kcal/mol respectively. As far as n to σ^* transitions are concerned the most intense transition in case of **C1** is present between LP (2) O_2 to $\sigma^* O_1-C_4$ with an interaction energy of 31.41 Kcal/mol in case of **C1**. The same group of orbitals are involved in n to σ^* in the rest of the molecules. The interaction energy between LP (2) O_2 to $\sigma^* O_1-C_4$ in **C2**, **C3**, **C4**, **C5** and **C6** are 31.41, 31.60, 31.59, 31.50 and 31.63 Kcal/mol respectively. The third significant interaction *i.e.*, n to π^* exists in between LP (2) O_1 to $\pi^* O_2-C_4$ with an interaction energy of 28.47 Kcal/mol. A similar pattern of n to π^* transition was observed for all the molecules except **C5** in which the most intense transition is from LP (2) O_1 to $\pi^* C_4-O_{12}$ with an interaction energy of 28.40 Kcal/mol. However, in case of **C2**, **C3**, **C4** and **C6** the interaction energy for LP (2) O_1 to $\pi^* O_2-C_4$ is 28.33, 28.20, 28.22 and 28.16 Kcal/mol respectively. The details of other intense interactions present in case of all the molecules has been provided in tables for Second order perturbation analysis for possible hyper conjugative interactions in six formyl coumarins (**C1-C6**) (**Table S1**)

2.2.3 Non-linear optical properties

Signal processing, optical interconnections and telecommunications are some of the established phenomenon, which are governed by optical materials, and hence development in this field is growing day by day³⁷⁻³⁹. The phase and frequency of electromagnetic waves alters when they interact with different media. These alterations resulted into non-linear optical properties in a molecule, which are expressed in terms of polarizability (α) and hyperpolarizability (β). DFT based methods are one of the inexpensive ways to predict NLO properties of any compound. First hyperpolarizability (β_o) is the basis of NLO properties exhibited by a molecule and molecular systems with higher first order hyperpolarizability (β_o) are associated with high NLO properties. The log file of Gaussian calculation consists of 10 components *i.e.*, β_{xxx} , β_{xyx} , β_{xyy} , β_{yyy} , β_{xxz} , β_{xyz} , β_{yyz} , β_{xzz} , β_{yzz} and β_{zzz} respectively of the $3 \times 3 \times 3$ matrix, from which three values of β for x, y and z components were calculated using the following equations.

$$\beta_x = \beta_{xxx} + \beta_{xyy} + \beta_{xzz}; \beta_y = \beta_{yyy} + \beta_{yzz} + \beta_{yxx} \text{ and } \beta_z = \beta_{zzz} + \beta_{zxx} + \beta_{zyy}$$

When reporting the single value of β , three independent value of β for x, y and z components are treated by quasi-Pythagorean problem and solve for average β by following equation.

$$\beta_{tot} = (\beta_x^2 + \beta_y^2 + \beta_z^2)^{1/2}$$

In the .log file, the value of β are reported in atomic units (a.u) and the values are converted into electrostatic units (esu) (1 a.u. = 8.6393×10^{-33}) and the value of $\langle \Delta \alpha \rangle$ are converted into electrostatic units (esu) (1 a.u. = 0.1482×10^{-24}). The value of (β_o) calculated for **C4** is 1.647×10^{-30} esu, which is 2 times greater than that for *p*-nitro aniline (PNA). The hyperpolarizability (β_o) for coumarin derivatives (**C1-C6**) are listed in **Table 7**.

Table 7. NLO properties of coumarin derivatives (**C1-C6**)

Compound	β	$\beta \times 10^{-30}$ (esu)	$\langle \Delta \alpha \rangle$	$\langle \Delta \alpha \rangle \times 10^{-24}$ (esu)
C1	398.110	0.398	30.830	4.569
C2	569.158	0.569	36.933	5.473
C3	418.725	0.419	25.082	3.717
C4	1647.28	1.647	28.590	4.237
C5	479.501	0.480	38.123	5.645
C6	403.340	0.403	22.068	3.270
PNA	739.895	0.740	15.883	2.354

2.2.4 Molecular electrostatic potential (MEP)

MEP is an important tool to identify the potential hydrogen bonding sites, electron density and electrophilic and nucleophilic centres⁴⁰. Some other properties like dipole moment, chemical reactivity and Electronegativity can also be predicted by using MEP. Same level of DFT theory was used to calculate MEP for optimized structure of all formyl coumarins. The different types of colors represent electrostatic potential. Where red color indicates the region of negative potential with high probability of electrophilic attacks whereas blue color represents potential. All the range of electrostatic potential are in between red and blue colors and follow the order: blue > green > white > orange > red. Over the examination of MEP plots, it is clear that oxygen and halogen atoms present in the molecules are carrying negative electrostatic potential and hence have maximum probability of electrophilic attack, and hydrogen atoms present on both rings of molecules are carrying positive electrostatic potential and hence have maximum probability of nucleophilic attack. Moreover, some carbon atoms in these molecules have the probability of nucleophilic attack (Fig. 10).

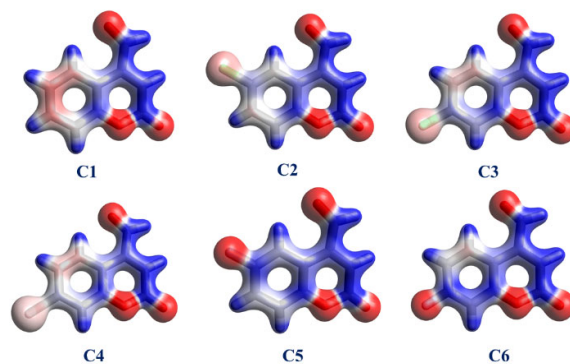


Fig. 10. MEP plots for substituted coumarin derivatives (C1 to C6)

3. Conclusion

The same range of d_i and d_e in all six formyl coumarins reflects the presence of good close packing and strong intermolecular interactions. Strong O-H interactions in all the coumarins revealed the presence of directional non-covalent hydrogen bonding which is responsible for molecular architecture. The probability of charge transfer with DNA have been explored using electrophilicity based charge transfer (ECT) analysis, which revealed the electrophilic behavior of substituted formyl coumarins over different DNA base pair *i.e.*, adenine, guanine, cytosine and thymine. Such behavior could help in the development of probes for quantification of DNA. The reactivity and selectivity of different coumarin derivatives was predicted by condensed Fukui functions. It has been revealed from second order Fock analysis that three types of interactions are more significant in case of all the molecules *i.e.*, π to π^* , n to σ^* and n to π^* . Over the examination of MEP plots, it is clear that oxygen and halogen atoms present in the molecules are carrying negative electrostatic potential.

4. Experimental

The crystal structure for different halogen substituted formyl coumarins selected for the present study has been retrieved from crystallographic centre for data collection (CCDC). Molecular Hirshfeld surfaces were generated using Crystal Explorer program (Version. 3.1) and analysis of intermolecular contacts were made using fingerprint plots. The structural and spectroscopic properties of the six different halogen substituted formyl coumarins were calculated using Gaussian 09 program. Density functional theory (DFT) with three-parameter hybrid correlation functional B3LYP and basis set 6-311++G (d,p) augmented by p polarization functions on hydrogen atoms and d polarization functions on Halogen atoms as well as diffuse functions for both hydrogen and halogen atoms were used. The geometry of six different halogen substituted formyl coumarins were optimized and confirmed based on absence of any imaginary vibrational frequency. Then, HOMO (Highest Occupied Molecular Orbital) and LUMO (Lowest Unoccupied Molecular Orbital) energy calculations were performed. In an attempt to calculate the adiabatic ionization potential (IP_A) and electron affinity (EA_A) for substituted coumarin derivatives. The structure of neutral, cationic and anionic coumarin derivatives (C1-C6) has been optimized using B3LYP/6-311G(+),d,p and CAM-B3LYP/6-311G(+),d,p level of theory, and their respective ionization potential and electron affinity was calculated using ΔE method. Avogadro 2.1 and Gauss sum were used for the visualization of the results. Same level of DFT theory was used to calculate MEP for optimized structure of all six molecules of formyl coumarin.

References

- Desiraju G. R. (2007) Crystal engineering: A holistic view. *Angew. Chemie - Int. Ed.*, 46, 8342–8356
- Kollman P. A. (1977) Noncovalent Interactions. *Acc Chem Res.*, 10, 365–371.
- Mooibroek T. J., Gamez P., Reedijk J. (2008) Lone pair- π interactions: A new supramolecular bond? *CrystEngComm.*, 10, 1501–1515.
- Arkas M., Kitsou I., Gkouma A., Papageorgiou M. (2019) The role of hydrogen bonds in the mesomorphic behaviour of supramolecular assemblies organized in dendritic architectures. *Liq Cryst Rev.*, 7, 60–105.
- Roesky H. W., Andruh M. (2003) The interplay of coordinative, hydrogen bonding and π - π stacking interactions in sustaining

- supramolecular solid-state architectures. A study case of *bis*(4-pyridyl)- and *bis*(4-pyridyl-N-oxide) tectons. *Coord Chem Rev.*, 236, 91–119.
6. Mason S. F. (1984) Origins of biomolecular handedness. *Nature.*, 311, 19–23.
 7. McClements D. J. (2006) Non-covalent interactions between proteins and polysaccharides. *Biotechnol Adv.*, 24, 621–625.
 8. Alkorta I., Grabowski S. J. (2012) Non-covalent interactions. *Comput. Theor. Chem.*, 998, 1
 9. Spackman M. A., Jayatilaka D. (2009) Hirshfeld surface analysis. *CrystEngComm* 11, 19–32. <https://doi.org/10.1039/b818330a>
 10. McKinnon J. J., Jayatilaka D., Spackman M. A., (2007) Towards quantitative analysis of intermolecular interactions with Hirshfeld surfaces. *Chem Commun.*, 3814–3816.
 11. Clausen H. F., Chevallier M. S., Spackman M. A., Iversen B. B., (2010) Three new co-crystals of hydroquinone: Crystal structures and Hirshfeld surface analysis of intermolecular interactions. *New J Chem.*, 34, 193–199.
 12. Spackman M. A., McKinnon J. J. (2002) Fingerprinting intermolecular interactions in molecular crystals. *CrystEngComm.*, 4, 378–392.
 13. Kohn W., Becke A. D., Parr R., G. (1996) Density functional theory of electronic structure. *J Phys Chem.*, 100, 12974–12980.
 14. Zhao Y., Truhlar D. G., (2007) Density functionals for noncovalent interaction energies of biological importance. *J Chem Theory Comput.*, 3, 289–300.
 15. Jasiński R., Mróz K., Kačka A. (2016) Experimental and Theoretical DFT Study on Synthesis of Sterically Crowded 2,3,3,(4)5-Tetrasubstituted-4-nitroisoxazolidines via 1,3-Dipolar Cycloaddition Reactions Between Ketonitrones and Conjugated Nitroalkenes. *J Heterocycl Chem.*, 53, 1424–1429.
 16. Hawkes K. J., Yates B. F. (2008) The mechanism of the Stetter reaction - A DFT study. *European J Org Chem.*, 5563–5570.
 17. Klein E., Lukeš V., Ilčin M. (2007) DFT/B3LYP study of tocopherols and chromans antioxidant action energetics. *Chem Phys.*, 336, 51–57.
 18. Stanton R. V., Merz K. M., (1994) Density functional study of symmetric proton transfers. *J Chem Phys.*, 101, 6658–6665.
 19. Kačka A., Jasiński R. (2017) A dramatic change of kinetic conditions and molecular mechanism of decomposition processes of nitroalkyl carboxylates catalyzed by ethylammonium cations. *Comput Theor Chem.*, 1104, 37–42.
 20. Siadati SA, Vessally E, Hosseinian A, Edjlali L (2016) Possibility of sensing, adsorbing, and destructing the Tabun-2D-skeletal (Tabun nerve agent) by C20 fullerene and its boron and nitrogen doped derivatives. *Synth Met* 220:606–611.
 21. Chattaraj P., K. (Ed.). (2009). *Chemical Reactivity Theory: A Density Functional View* (1st ed.). CRC Press.
 22. Torrent-Sucarrat M., De Proft F., Ayers P., W., Geerlings P. (2010) On the applicability of local softness and hardness. *Phys Chem Chem Phys.*, 12, 1072–1080.
 23. Zhu M., Ge F., Zhu R., et al., (2010) A DFT-based QSAR study of the toxicity of quaternary ammonium compounds on *Chlorella vulgaris*. *Chemosphere.*, 80, 46–52.
 24. Casida M., E. (2009) Time-dependent density-functional theory for molecules and molecular solids. *J. Mol. Struct. THEOCHEM.*, 914, 3–18
 25. Burke K., Werschnik J., Gross E., K., U. (2005) Time-dependent density functional theory: Past, present, and future. *J Chem Phys.*, 123
 26. Fabian J. (2010) TDDFT-calculations of Vis/NIR absorbing compounds. *Dyes & Pigment.*, 84, 36–53.
 27. Garza A. J., Osman O. I., Wazzan N. A., et al (2014) A computational study of the nonlinear optical properties of carbazole derivatives: Theory refines experiment. *Theor Chem Acc.*, 133, 1–8.
 28. Nagaraj R., Ramachandran K., Aravindh K., Ranjith S. (2020) Investigation on structural, optical, thermal and mechanical properties of 1, 3-dinitrobenzene (1,3-DNB) single crystal. *J Mol Struct*, 1205:
 29. Chattaraj P. K., Giri S. (2009) Electrophilicity index within a conceptual DFT framework. *Annu. Reports Prog. Chem.-Sect. C.*, 105, 13–39
 30. Roy R. K. (2004) On the reliability of global and local electrophilicity descriptors. *J Phys Chem A.*, 108, 4934–4939.
 31. Padmanabhan J., Parthasarathi R., Subramanian V., Chattaraj P. K. (2007) Electrophilicity-based charge transfer descriptor. *J Phys Chem A.*, 111, 1358–1361.
 32. Thanikaivelan P., Padmanabhan J., Subramanian V., Ramasami T. (2002) Chemical reactivity and selectivity using Fukui functions: Basis set and population scheme dependence in the framework of B3LYP theory. *Theor Chem Acc.*, 107, 326–335.
 33. Oláh J., Alsenoy C. Van, Sannigrahi A. B. (2002) Condensed Fukui functions derived from stockholder charges: Assessment of their performance as local reactivity descriptors. *J Phys Chem A*, 106, 3885–3890.
 34. Glendening E. D., Landis C. R., Weinhold F. (2013) NBO 6.0: Natural bond orbital analysis program. *J Comput Chem.*, 34, 1429–1437.
 35. Weinhold F (2012) Natural bond orbital analysis: A critical overview of relationships to alternative bonding perspectives. *J. Comput. Chem.*, 33, 2363–2379
 36. Freitas M. P., (2013) The anomeric effect on the basis of natural bond orbital analysis. *Org Biomol Chem.*, 11, 2885–2890.
 37. Balanay M. P., Kim D. H. (2011) Optical properties of porphyrin analogues for solar cells: An NLO approach. *Curr Appl Phys.*, 11:109–116.
 38. Liyanage P. S., De Silva R. M., De Silva K. M. N. (2003) Nonlinear optical (NLO) properties of novel organometallic complexes: High accuracy density functional theory (DFT) calculations. *J Mol Struct THEOCHEM.*, 639, 195–201.
 39. Liu C. G., Qiu Y. Q., Sun S. L., et al (2006) DFT study on second-order nonlinear optical properties of a series of mono Schiff-base M(II) (M = Ni, Pd, Pt) complexes. *Chem Phys Lett.*, 429, 570–574.
 40. Grimme S. (1998) Molecular Electrostatic Potentials: Concepts and Applications. *Zeitschrift für Phys Chemie.*, 205, 136–137.

